Optimal Bidding of EV Aggregators in Joint Energy and Frequency Markets Under Uncertainty Based on Problem-Driven Scenario Reduction

Yu Yang, *Member, IEEE,* Boning Zhao, Qing-Shan Jia, *Senior Member, IEEE,* Lun Yang, *Member, IEEE,* Zhenyu Pu, Xiaohong Guan, *Life Fellow, IEEE*

***Abstract*—As both significant electrical load and substantial flexible resources, EV charging stations or aggregators can participate in both energy and frequency markets to gain economic benefits. However, their optimal bidding is challenged by the difficulty to capture the market capacity aggregated from large-scale EVs under heterogeneous user driving behaviors, as well as the computational complexity introduced by scenario-based uncertainty modeling. To address the challenges, an aggregated multi-time-scale bidding model was proposed for charging station by leveraging an aggregated virtual battery model (VES) to capture the market capability of EVs and meanwhile incorporating both the temporal and hierarchical couplings for joint market participation. A problem-driven scenario reduction method is further proposed to address the computational complexity while improving bidding strategies. Unlike conventional methods, the proposed method guides informed scenario selection by incorporating downstream bidding optimization problem into consideration. Case studies based on real-world datasets demonstrate that the proposed problem-driven method provides approximately 10-20% of market performance improvement over conventional methods. Besides, substantial economic benefits (i.e., over 45%) can be gained from the joint market participation over single market participation. Further, some intuitive explanations regarding the problem-driven method are investigated. The results show that the problem-driven method is able to capture the collective impacts of multiple uncertainties on the downstream bidding problem and thereby improve bidding strategies, which are not provided by the conventional methods.**

***Index Terms*—EV charging station, joint energy and frequency market, optimal bidding, problem-driven scenario reduction, aggregated and multi-time-scale bidding model**

I. Introduction

ELECTRIC vehicles (EVs) are undergoing profound growth around the world. Over the past decade, the global stock of electric cars has reached 58 million, accounting for 4% of passenger fleet. Almost one of ten light-duty vehicles sold in US and nearly half car sales in China are now electric [1]. EVs represent significant increasing electrical load of global power systems. For example, the PJM interconnection, a regional transmission organization (RTO) of US forecasts that the EV growth will contribute to around 7% and 9% of the region's peak and total electrical loads by 2046 [2]. Meanwhile, EVs represent substantial flexible resources of modern power systems. EV charging demand can be flexibly shifted across time and the emerging vehicle-to-grid (V2G) even allows EVs to work as distributed energy storage system when connected. As both huge electrical loads and flexible resources, EV charging stations or aggregators have been recognized as important market players of future power systems. Specifically, through aggregation or virtual power plant (VPP) technologies, EVs are able to participate in both energy and ancillary service markets to gain economic benefits and provide extensive balancing services to modern power system. This is critical both to address the impacts of uncontrolled EV charging demand and the shortage of flexible resources of modern power system to accommodate the increasing volatile renewable penetration. In recent years, the boosting of smart vehicle-grid integration platforms, such as US Cascade EV Aggregator [3] and California ev.energy [4] have further facilitated the aggregation of EVs to behave actively in electricity markets.

For market participation, one of the critical issues is enable the optimal bidding of EV charging station or aggregators in electricity markets. Specifically, the charging station or aggregators are required to submit their trading quantities and prices (i.e., bids) for all trading intervals of following day. The bidding strategies not only determine whether the bids will be cleared (i.e., accepted) but also how they will be rewarded. Moreover, the participants are better to comply with committed bids if cleared, otherwise it will incur substantial economic penalties or deteriorate their market credibility. While critical, the optimal bidding of charging stations or aggregators represents a challenging issue. *First*, their market capabilities are aggregated from individual vehicles under heterogeneous user driving behaviors. It is difficult to fully capture the market capabilities for large-scale connected vehicles. *Besides*, there exist multiple uncertainties, including the fluctuating market clearing prices and the uncertain EV charging demand characterized by random arrival and departure time, as well as required charging energy, which are not often known at the day-ahead bidding stage.

In the literature, many efforts have been devoted to es-

This work is supported by the National Natural Science Foundation of China (62403373, 72595834, 62192752).

Y. Yang, B. Zhao, L. Yang and Z. Pu are with School of Automation Science and Engineering, Xi'an Jiaotong University, Shaanxi, China (e-mail: yangyu21@xjtu.edu.cn). *Y. Yang is the corresponding author.*

Q. -S. Jia is with the Center for Intelligent and Networked Systems, Department of Automation, BNRist, Tsinghua University, Beijing 100084, China (e-mail: jiaqs@tsinghua.edu.cn).

X. Guan is with School of Automation Science and Engineering, Xi'an Jiaotong University, Shaanxi, Xi'an 710049, China, and also with the Center for Intelligent and Networked Systems, Department of Automation, Tsinghua University, Beijing 100084, China (e-mail: xhguan@tsinghua.edu.cn).

tablishing bidding models of EVs in electricity markets. For example, Matkovic et al. [5] investigated the optimal bidding of EV charging station in day-ahead energy market by treating charging demand as uncontrollable load. Wang et al. [6] studied the optimal bidding of a V2G aggregator in day-ahead energy markets based on a detailed battery model. Baringo et al. [7, 8] studied the optimal bidding of an EV aggregator in day-ahead energy market by an aggregated charging model. Further, Chen et al. [9] studied the optimal bidding of an EV aggregator in joint energy and frequency markets, where the market capability of each individual vehicle was explicitly modeled. Sadeghi et al. [10] studied the optimal bidding of VPP in joint energy and frequency markets. Notably, a multi-time-scale bidding model was proposed to capture both the temporal and hierarchical couplings of joint market participation. Gao et al. [11] studied the optimal bidding of an EV fleet in joint energy and frequency market by an aggregated EV charging model. However, this work mainly focused on investigating the economic benefits of EV fleet instead of optimizing the bidding strategies under uncertainty. Despite these research progress, many important issues remain to be addressed. In particular, existing works mainly depend on the charging and discharging model of individual vehicles to capture their aggregated market capability. Though accurate, the resulting bidding models are often associated with high-dimensional constraints and decision variables, making them not scalable to large-scale vehicles. In addition, the multi-time-scale nature of joint market participation has not been well addressed. Specifically, wholesale markets are often operated at longer trading interval and retail (real-time) markets are often at much shorter trading intervals. This leads to bidding decisions coupled across different time scales. To accommodate the increasing number of EVs and enable profitable market participation, it is important to develop scalable and joint bidding models for charging stations or aggregators.

Another common challenge for the optimal bidding of market players is the multiple uncertainties. In the literature, scenario-based stochastic programming (SP) [12–15], forecasting-based methods [10, 16], and stochastic robust optimization (SRO) [17] have been investigated to address the uncertainties. While forecasting-based methods are applicable when the uncertainties can be predicted relatively accurately, SROs are particularly suitable for cases with limited information on the uncertainties and emphasizing risks on market performances. Among them, scenario-based SP have been widely used due to its effectiveness to handle non-analytical uncertainties and does not result in overly conservative bidding strategies. While scenario-based SP can effectively use scenarios or historical realizations to capture the uncertainties, the associated computational complexity caused by the scenario-based formulation represents a key challenge. Scenario reduction or selection methods were used in many existing works to mitigate the computational complexity. However, the market performance of the resulting bidding strategies is often limited. This is primarily because most scenario selection or reduction methods [18–21] select scenarios in the original uncertainty space and do not account for the target scenario-based SP problem. The optimal solutions to SP are often jointly affected by multiple uncertainties. Selecting scenarios in the original uncertainty space by minimizing probability distances or statistical characterization discrepancies of scenario sets does not necessarily lead to the optimal solution of downstream SP. The limitation has been recognized particularly significant with power system related applications suffering from multiple sources of uncertainties [22–24]. To address this limitation, some recent works explored the incorporation of downstream SP into scenario selection. For example, Zhuang et al. [23] proposed to evaluate the distance of scenarios by the induced SP performance instead of probability distances to improve SP performance. Suemitsu et al. [24] proposed a cost-based scenario generation by a cost-based distance metric for evaluating scenario similarity instead of conventional probability distances. While these problem-driven scenario reduction methods were demonstrated promising to improve the decision performance, they are not directly applicable to the optimal bidding problem either due to the problem-specific feature or the high computational complexity.

Motivated by the above research gaps, this paper studies the optimal bidding of EV charging station in the joint energy and frequency markets under uncertainty. Our main contributions are summarized as follows.

- We propose an aggregated multi-time-scale model for the optimal bidding of charging station in joint energy and frequency market under uncertainty. The model leverages an aggregated virtual battery model (VES) to capture the collective market capabilities of EVs, as well as incorporates both the temporal and hierarchical couplings of joint market participation.
- We further propose a problem-driven scenario reduction method to address the computational complexity of the bidding optimization problem while improving bidding strategies. Different from conventional methods, the method guides informed scenario selection by incorporating downstream bidding optimization problem into account and thereby improving bidding strategies.

Case studies based on real-world datasets show that the propose problem-driven scenario reduction method provides approximately 10-20% of market performance improvement over conventional methods. Besides, the charging station can gain substantial enhanced economic benefits (i.e., over 45%) from the joint market participation over the single energy market participation. Some intuitive explanations regarding the effectiveness of the proposed scenario reduction method are investigated. The results imply that the proposed problem-driven method is able to capture the collective impacts of the multiple uncertainties on the downstream bidding problem and thus improve the bidding strategies, which are not provided by the conventional scenario reduction method.

The remainder of this paper is as follows. Section II presents the aggregated multi-time-scale bidding model of EV charging station in the joint energy and frequency markets. Section III introduces the problem-driven scenario reduction method. Section IV presents the numerical results of case studies. Section V concludes this paper.

II. EV Charging Station Jointly Participates in Energy and Frequency Markets

A. Overview of the EV charging station

As illustrated in Fig. 1, an electric vehicle (EV) charging station serving commuted vehicles within a commercial area is considered. The vehicles are classified into uni-directional EVs and bi-directional V2Gs, where the former can only get charged and the latter can both charge and discharge when connected. While providing charging service, the charging station is authorized to participate in electricity markets to gain economic benefits. The on-site PV generators on top of the buildings are connected to the charging station for supplying the charging demand and enhancing the market capability. For market participation, the VPP operator on behalf of the charging station is required to submit the bids (i.e., trading quantities and prices) for all trading intervals of the following day to the market operator. This paper investigates the optimal bidding of the charging station in the joint energy and frequency markets, including day-ahead and real-time energy markets as well as frequency market. Day-ahead energy and frequency markets are generally operated on hourly basis, and real-time energy market is generally cleared every 5 or 15 mins. Therefore, the problem corresponds to a multi-time-scale decision problem.

Notations: Throughout the paper, the superscripts `e`, and `reg` indicate energy and frequency market, the superscript `bid` denotes bidding quantities. A positive bid means selling energy or regulation capacity in markets, and vice versa.

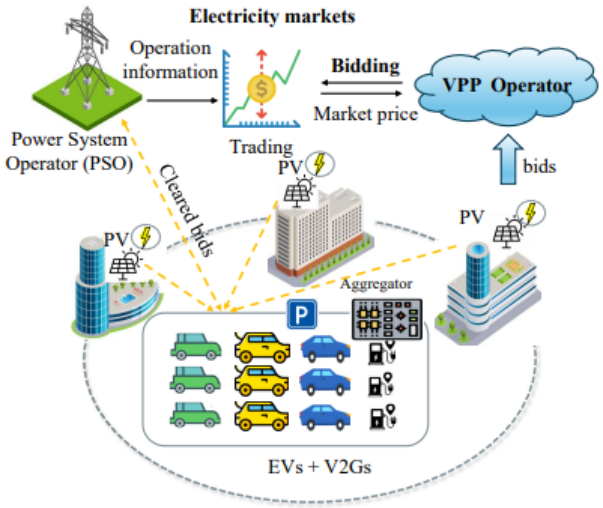

Fig. 1. An EV charging station participates in electricity markets

B. An aggregated multi-time-scale bidding model

To capture the multi-time-scale nature of joint market participation, we use t and τ to denote the trading indices of day-ahead and real-time markets. The corresponding trading intervals are denoted as Δt and $\Delta\tau$. It is worth noting that each day-ahead trading interval corresponds to multiple real-time trading intervals. The time horizon of a whole day is denoted by T. The multiple uncertainties associated with the joint market bidding are considered, which includes market prices, solar generation and charging demand. Considering the non-analytical nature of these uncertainties, a scenario set $\boldsymbol{\xi}=\{\xi_1,\xi_2,\cdots,\xi_S\}$ formed by the historical realizations of these uncertain variables together with the probability distribution $\boldsymbol{P}=[p_1,p_2,\cdots,p_s]$ is used to capture these uncertainties. We denote the scenario indices as $S=\{1,2,\cdots,S\}$. To hedge against the impacts of multiple uncertainties, step-wise bidding curves consisting of a number of quantity-price pairs for each trading interval are optimized. The optimal bidding problem is formulated as a scenario-based SP. Particularly, the market capability of the charging station is aggregated from the on-site PV generator and connected vehicles, and a bottom-up modeling framework is thus adopted.

1) PVs: The market capability of PV units in the joint energy and frequency markets are determined by their available outputs. For each scenario s with hourly and real-time maximum PV outputs $P_{s,t}^{\mathrm{PV}}$ and $P_{s,\tau}^{\mathrm{PV}}$, the joint market behaviors of PV units can be modeled as

$$0\le P_{s,t}^{\mathrm{e,PV,bid}}\le P_{s,t}^{PV}, \tag{1a}$$

$$0\le P_{s,\tau}^{\mathrm{e,PV}}\le P_{s,\tau}^{\mathrm{PV}}, \tag{1b}$$

$$0\le P_{s,t}^{\mathrm{reg,PV,up}}\le P_{s,t}^{\mathrm{PV}}-P_{s,\tau}^{\mathrm{e,PV}}, \tag{1c}$$

$$0\le P_{s,t}^{\mathrm{reg,PV,dn}}\le P_{s,\tau}^{\mathrm{e,PV}},\forall\tau\in[t,t+\Delta t),\ t\in T. \tag{1d}$$

where $P_{s,t}^{\mathrm{e,PV,bid}}$ and $P_{s,\tau}^{\mathrm{e,PV}}$ denote the quantity that the PV units bid to trade in day-ahead and real-time energy markets for trading indices t and τ. As modeled in (1a)-(1b), these bidding quantities are upper bounded by the maximum available PV generation. $P_{s,t}^{\mathrm{reg,PV,up}}$ and $P_{s,t}^{\mathrm{reg,PV,dn}}$ denote the upward and downward frequency regulation capacity that are available from the PV units, which are non-negative and upper bounded. Specifically, as pure generators, PV units can only provide regulation capacity through increasing or decreasing outputs as characterized by (1c) and (1d).

2) V2G and EV aggregators: To accommodate a large number of connected vehicles, aggregated models for capturing the collective market behaviors of V2Gs and EVs are proposed. Aggregated models are preferred for bidding as only the system-level operating boundaries are required at the bidding stage. In particular, the virtual energy storage (VES) models developed in our previous work [25] are leveraged to characterize the aggregated charging and discharging flexibility of V2Gs and EVs. For V2Gs, the proposed VES model describing the feasible aggregated charging and discharging region is

$$\begin{cases} 0\le P_{\tau}^{\mathrm{V2G,agg,ch}}\le P_{\tau}^{\mathrm{V2G,agg,ch,max}}, \\ 0\le P_{\tau}^{\mathrm{V2G,agg,dis}}\le P_{\tau}^{\mathrm{V2G,agg,dis,max}}, \\ L_{\tau}^{\mathrm{V2G,agg}}=L_{\tau-1}^{\mathrm{V2G,agg}}+\left(P_{\tau}^{\mathrm{V2G,agg,ch}}\eta^{\mathrm{ch}}-\dfrac{P_{\tau}^{\mathrm{V2G,agg,dis}}}{\eta^{\mathrm{dis}}}\right)\Delta\tau, \\ L_{\tau}^{\mathrm{V2G,agg,min}}\le L_{\tau}^{\mathrm{V2G,agg}}\le L_{\tau}^{\mathrm{V2G,agg,max}},\forall\tau\in[t,t+\Delta t),t\in T. \end{cases} \tag{2}$$

where $P_t^{\mathrm{V2G,agg,ch/dis,max}}$ and $L_t^{\mathrm{V2G,agg,min/max}}$ are aggregated maximum charging/discharging power and the lower/upper bounds of accumulative net charging energy of the V2Gs. $P_t^{\mathrm{V2G,agg,ch/dis}}$ are scheduled aggregated charging/discharging power to the V2Gs. $L_t^{\mathrm{V2G,agg}}$ denote the accumulative net charging energy of the V2Gs up to time t. $\eta^{\mathrm{ch/dis}}$ denote the

homogeneous charging/discharging efficiencies of V2Gs. It is worth noting that the VES model (2) proposes a general aggregated charging and discharging scheduling model for V2Gs considering charging requirements and battery operating limits of all individual V2Gs. $P_t^{\text{V2G,agg,ch/dis,max}}$ and $L_t^{\text{V2G,agg,min/max}}$ can be viewed as time-dependent power and energy capacity of the VES. They are model parameters and can be obtained from the charging requirements and battery parameters of individual V2Gs. The details to obtain the VES models for both EVs and V2Gs can refer to our previous work [25].

While participating in electricity markets, the VES model (2) should be adapted to incorporate the multi-time-scale coordination across the electricity markets and the uncertain charging requirements. Specifically,based on the VES model (2), the market behaviors of a V2G aggregator in joint energy and frequency markets can be modeled as

$$P_{s,t}^{\text{e,V2G,agg,bid}}, P_{s,\tau}^{\text{e,V2G,agg}} \in R, \tag{3a}$$
$$P_{s,t}^{\text{reg,V2G,agg,up}}, P_{s,t}^{\text{reg,V2G,agg,dn}} \geq 0, \tag{3b}$$
$$P_{s,t}^{\text{reg,V2G,agg,up}} \leq P_{s,\tau}^{\text{V2G,agg,dis,max}} - P_{s,\tau}^{\text{e,V2G,agg}}, \tag{3c}$$
$$P_{s,t}^{\text{reg,V2G,agg,dn}} \leq P_{s,\tau}^{\text{V2G,agg,ch,max}} + P_{s,\tau}^{\text{e,V2G,agg}}, \tag{3d}$$
$$L_{s,\tau-1}^{\text{V2G,agg}} - (P_{s,\tau}^{\text{e,V2G,agg}} + P_{s,t}^{\text{reg,V2G,agg,up}})\Delta\tau/\eta^{\text{dis}} \geq L_{s,\tau}^{\text{V2G,agg,min}}, \tag{3e}$$
$$L_{s,\tau-1}^{\text{V2G,agg}} + (P_{s,t}^{\text{reg,V2G,agg,dn}} - P_{s,\tau}^{\text{e,V2G,agg}})\eta^{\text{ch}}\Delta\tau \leq L_{s,\tau}^{\text{V2G,agg,max}}, \tag{3f}$$
$$\forall \tau \in [t, t+\Delta t), t \in T.$$

where $P_{s,t}^{\text{e,V2G,agg,bid}}$ and $P_{s,\tau}^{\text{e,V2G,agg}}$ denote the quantities that the V2G aggregator bid to trade in day-ahead and real-time energy markets for trading indices t and τ. Since V2Gs are capable of charging and discharging, the aggregator can bid to buy or sell in energy markets as modeled in (3a). $P_{s,t}^{\text{reg,V2G,agg,up/dn}}$ denote the upward/downward frequency regulation capacity available from the V2G aggregator, which are non-negative as indicated in (3b). As a prosumer, the V2G aggregator can provide upward frequency regulation either through decreasing charging or increasing discharging, and vice verse for downward regulation. The available upward and downward regulation capacities are bounded by the remaining discharging and charging power capacity of the aggregator accounting for real-time energy market schedules as modeled in (3c) and (3d). They are also constrained by the energy state and capacity of the V2G aggregator at the beginning of each trading instance. Specifically, the remaining dispatchable energy should be sufficient to support both upward frequency regulation and real-time energy market schedule for each trading interval as modeled in (3e). For downward frequency regulation, it requires that the remaining energy capacity is enough to accommodate the charging requirement of frequency regulation and real-time energy market transaction as modeled in (3f).

EVs can be viewed as a special case of V2Gs that are only allowed to get charged when connected. Therefore, similar VES model can be obtained for capturing the aggregated charging flexibility of EVs given their charging requirements. This can be achieved by directly setting the maximum maximum discharging power $P_\tau^{\text{V2G,agg,dis,max}}$ to be *zero* with the VES model (2). Accordingly, the model for characterizing the market behaviors of EV aggregator can be directly adapted from the model (3) for V2Gs, and we have

$$P_{s,t}^{\text{e,EV,agg,bid}}, P_{s,\tau}^{\text{e,EV,agg}} \leq 0, \tag{4a}$$
$$P_{s,t}^{\text{reg,EV,agg,up}}, P_{s,t}^{\text{reg,EV,agg,dn}} \geq 0, \tag{4b}$$
$$P_{s,t}^{\text{reg,EV,agg,up}} \leq -P_{s,\tau}^{\text{e,EV,agg}}, \tag{4c}$$
$$P_{s,t}^{\text{reg,EV,agg,dn}} - P_{s,\tau}^{\text{e,EV,agg}} \leq P_{s,\tau}^{\text{EV,agg,ch,max}}, \tag{4d}$$
$$L_{s,\tau-1}^{\text{EV,agg}} - (P_{s,\tau}^{\text{e,EV,agg}} + P_{s,t}^{\text{reg,EV,agg,up}})\Delta\tau \geq L_{s,\tau}^{\text{EV,agg,min}}, \tag{4e}$$
$$L_{s,\tau-1}^{\text{EV,agg}} + (P_{s,t}^{\text{reg,EV,agg,dn}} - P_{s,\tau}^{\text{e,EV,agg}})\eta^{\text{ch}}\Delta\tau \leq L_{s,\tau}^{\text{EV,agg,max}}, \tag{4f}$$
$$\forall \tau \in [t, t+\Delta t), t \in T.$$

where the above model is directly adapted from (3) with the maximum charging/discharging power setting to be *zero*. The notations are directly adapted from that of the V2G aggregator. One slight difference is that the EV aggregator is a pure energy consumer and can only bid to buy in energy markets as modeled in (4a). Besides, it is worthy noting that the EV aggregator can only provide frequency regulation through increasing or decreasing charging power.

3) VPP operator: On behalf of the charging station, the VPP operator bids in the joint energy and frequency markets. The bidding quantities are defined as $P_{s,t}^{\text{e,VPP,bid}}, t \in T$ for day-ahead energy market, $P_{s,\tau}^{\text{e,VPP}}, \tau \in [t, t+\Delta t), t \in T$ for real-time energy market, $P_{s,t}^{\text{reg,VPP,up}}, P_{s,t}^{\text{reg,VPP,dn}}, t \in T$ for frequency market. These bidding quantities are aggregated from the flexible resources of the charging station and we thus have the consistency constraints:

$$\begin{aligned}
P_{s,t}^{\text{e,VPP,bid}} &= P_{s,t}^{\text{e,PV,bid}} + P_{s,t}^{\text{e,EV,agg,bid}} + P_{s,t}^{\text{e,V2G,agg,bid}}, \\
P_{s,\tau}^{\text{e,VPP}} &= P_{s,\tau}^{\text{e,PV}} + P_{s,\tau}^{\text{e,EV,agg}} + P_{s,\tau}^{\text{e,V2G,agg}}, \\
P_{s,t}^{\text{reg,VPP,up}} &= P_{s,t}^{\text{reg,PV,up}} + P_{s,t}^{\text{reg,EV,agg,up}} + P_{s,t}^{\text{reg,V2G,agg,up}}, \\
P_{s,t}^{\text{reg,VPP,dn}} &= P_{s,t}^{\text{reg,PV,dn}} + P_{s,t}^{\text{reg,EV,agg,dn}} + P_{s,t}^{\text{reg,V2G,agg,dn}}, \\
&\forall \tau \in [t, t+\Delta t), t \in T.
\end{aligned} \tag{5}$$

Market rules: Many electricity markets impose limits on the deviation of day-ahead commitments and real-time transaction for stabilizing market prices. This can be captured by the following constraints:

$$\begin{aligned}
-P^{\text{e,dev,max}} \leq P_{s,t,\tau}^{\text{e,VPP}} - P_{s,t}^{\text{e,VPP,bid}} \leq P^{\text{e,dev,max}}, \\
\forall \tau \in [t, t+\Delta t),\ t \in T.
\end{aligned} \tag{6}$$

where $P^{\text{e,dev,max}}$ denotes the maximum allowable deviation of day-ahead and real-time energy market bidding and is typically a fixed proportion of day-ahead bidding (e.g., 40%).

In addition, many frequency market only accept symmetric frequency regulation bids to ensure balanced upward and downward frequency regulation capabilities. In such context, the frequency regulation bid $P_{s,t}^{\text{VPP,reg,bid}}$ is determined by

$$\begin{aligned}
0.5P_{s,t}^{\text{reg,VPP,bid}} &\leq P_{s,t}^{\text{reg,VPP,up}}, \\
0.5P_{s,t}^{\text{reg,VPP,bid}} &\leq P_{s,t}^{\text{reg,VPP,dn}}, \\
P_{s,t}^{\text{reg,VPP,bid}} &\geq 0, \forall t \in T.
\end{aligned} \tag{7}$$

Market Revenues: For joint energy and frequency market participation, the market revenue consists of energy and frequency market revenues. Energy market revenue is further can be divided into day-ahead energy market revenue $W_{s,t}^{\text{e,da}}$,

real-time energy market revenue $W_{s,t}^{\mathrm{e,rt}}$ and bidding deviation penalty cost $W_{s,t}^{\mathrm{e,penalty}}$, which are settled by

$$\begin{aligned}
&W_{s,t}^{\mathrm{e,da}} = m_{s,t}^{\mathrm{e}} \cdot P_{s,t}^{\mathrm{e,VPP,bid}} \cdot \Delta t \\
&W_{s,t}^{\mathrm{e,rt}} = \sum\nolimits_{\tau\in[t,t+\Delta t)} m_{s,\tau}^{\mathrm{e,rt}} \cdot \left(P_{s,\tau}^{\mathrm{e,VPP}} - P_{s,t}^{\mathrm{e,VPP,bid}}\right) \cdot \Delta\tau \\
&W_{s,t}^{\mathrm{e,penalty}} = \sum\nolimits_{\tau\in[t,t+\Delta t)} \pi_{\tau}^{\mathrm{e}} \cdot m_{s,\tau}^{\mathrm{e,rt}} \cdot \left|P_{\tau}^{\mathrm{e,VPP}} - P_{s,t}^{\mathrm{e,VPP,bid}}\right| \cdot \Delta\tau
\end{aligned} \tag{8}$$

where $m_{s,t}^{\mathrm{e}}$, $m_{s,\tau}^{\mathrm{e,rt}}$ are day-ahead and real-time energy market clearing prices. $\pi_{\tau}^{\mathrm{e}} \in [0,1]$ is a penalty factor imposing on the deviations of day-ahead commitments and real-time transactions, which is adopted by many electricity markets to incentive day-ahead energy scheduling. Both day-ahead and real-time energy market revenues are settled by the market clearing prices and trading quantities.

The frequency market revenue consists of capacity revenue $W_{s,t}^{\mathrm{reg,cap}}$ and performance revenue $W_{s,t}^{\mathrm{reg,perf}}$, which are

$$\begin{aligned}
&W_{s,t}^{\mathrm{reg,cap}} = m_{s,t}^{\mathrm{reg,cap}} \cdot P_{s,t}^{\mathrm{reg,VPP,bid}} \cdot K_{t}^{\mathrm{perf}} \cdot \Delta t \\
&W_{s,t}^{\mathrm{reg,perf}} = m_{s,t}^{\mathrm{reg,perf}} \cdot P_{s,t}^{\mathrm{reg,VPP,bid}} \cdot R \cdot K_{t}^{\mathrm{perf}} \cdot \Delta t
\end{aligned} \tag{9}$$

where $m_{t}^{\mathrm{reg,cap}}, m_{t}^{\mathrm{reg,perf}}$ are capacity and performance prices of frequency market. R denote the mileage ratio of the regulation signal, capturing the temporal variability. K_{t}^{perf} is the performance factor indicating a market player's average performance of following dynamic frequency regulation signals.

Step-wise Bidding Strategies: To hedge against the impacts of uncertainties on bidding performance, step-wise bidding curves formed by a number of bidding quantity-price pairs for each trading interval are optimized. It is worth noting that both single bidding quantities and flexible step-wise bidding curves are allowed by many electricity markets. According to [13, 14], the step-wise bidding curves should satisfy three structural properties: 1) monotonicity: For each trading interval, the bidding quantity is non-decreasing w.r.t. market price for selling and non-increasing for buying; 2) nonanticipativity: for each trading interval, the bidding quantity should be identical for the scenarios with same market clearing prices; and 3) segment limits: the maximum number of bidding quantity-price pairs allowed by market operator is limited. The following model is used to characterize the properties of step-wise bidding curves for energy and frequency markets.

Day-ahead energy market buying curve

$$\begin{aligned}
&Q_{s,t}^{\mathrm{e,bu}} = \Delta Q_{s,t}^{\mathrm{e,bu}}, \quad \forall s : O_{s,t}^{\mathrm{e}} = O_{t}^{\mathrm{e,max}}. \\
&Q_{s,t}^{\mathrm{e,bu}} = Q_{s',t}^{\mathrm{e,bu}} + \Delta Q_{s,t}^{\mathrm{e,bu}}, \quad \forall s, s', \\
&\qquad \forall O_{s',t}^{\mathrm{e}} = O_{s,t}^{\mathrm{e}} + 1 \wedge 1 < O_{s',t}^{\mathrm{e}} \le O_{t}^{\mathrm{e,max}}. \\
&Q_{s,t}^{\mathrm{e,bu}} = Q_{s',t}^{\mathrm{e,bu}}, \quad \forall s \ne s', t : m_{s,t}^{\mathrm{e}} = m_{s',t}^{\mathrm{e}}. \\
&\Delta Q^{\min} \cdot Y_{s,t}^{\mathrm{e,bu}} \le \Delta Q_{s,t}^{\mathrm{e,bu}} \le \Delta Q^{\max} \cdot Y_{s,t}^{\mathrm{e,bu}}, \forall s. \\
&Y_{s,t}^{\mathrm{e,bu}} \in \{0,1\}, \forall s. \quad \sum\nolimits_{s} Y_{s,t}^{\mathrm{e,bu}} \le N^{\mathrm{e,bu}}.
\end{aligned} \tag{10}$$

Day-ahead energy and frequency market selling curve

$$\begin{aligned}
&Q_{s,t}^{\mathrm{e/reg,se}} = \Delta Q_{s,t}^{\mathrm{e/reg,se}}, \ \forall s : O_{s,t}^{\mathrm{e/(reg,cap)}} = 1. \\
&Q_{s,t}^{\mathrm{e/reg,se}} = Q_{s',t}^{\mathrm{e/reg,se}} + \Delta Q_{s,t}^{\mathrm{e/reg,se}}, \quad \forall s, s', \\
&\forall O_{s',t}^{\mathrm{e/reg}} = O_{s,t}^{\mathrm{e/reg}} + 1 \wedge 1 < O_{s',t} \le O_{t}^{\mathrm{e/(reg,cap),max}}. \\
&Q_{s,t}^{\mathrm{e/reg,se}} = Q_{s',t}^{\mathrm{e/reg,se}}, \ \forall s \ne s', t : m_{s,t}^{\mathrm{e}} = m_{s',t}^{\mathrm{e/reg}}. \\
&\Delta Q^{\min} \cdot Y_{s,t}^{\mathrm{e/reg,se}} \le \Delta Q_{s,t}^{\mathrm{e/reg,se}} \le \Delta Q^{\max} \cdot Y_{s,t}^{\mathrm{e/reg,se}}, \forall s. \\
&Y_{s,t}^{\mathrm{e/reg,se}} \in \{0,1\}, \forall s. \quad \sum\nolimits_{s} Y_{s,t}^{\mathrm{e/reg,se}} \le N^{\mathrm{e/reg,se}}.
\end{aligned} \tag{11}$$

where to enforce the monotonicity, the market prices for each trading intervals of all scenarios are first sorted in non-decreasing manner and indexed by $O_{s,t}^{\mathrm{e}} \in \{1,2,\cdots,O_{t}^{\mathrm{e,max}}\}$ for energy market and $O_{s,t}^{\mathrm{reg,cap}} \in \{1,2,\cdots,O_{t}^{\mathrm{reg,cap,max}}\}$ for frequency market. $\Delta Q_{s,t}^{\mathrm{e,bu}}$, $\Delta Q_{s,t}^{\mathrm{e,se}}$ and $\Delta Q_{s,t}^{\mathrm{reg,se}}$ are increments imposed to ensure monotonicity of the step-wise bidding curves. The maximum segments of step-wise bidding curves are set as $N^{\mathrm{e,bu}}$, $N^{\mathrm{e,se}}$ and $N^{\mathrm{reg,se}}$, respectively. The segment limits of bidding curves are achieved by limiting the number of binary decision variables $Y_{s,t}^{\mathrm{e,bu}}$, $Y_{s,t}^{\mathrm{e,se}}$ and $Y_{s,t}^{\mathrm{reg,se}}$ to be active. $\Delta Q^{\min}$ and $\Delta Q^{\max}$ are minimum and maximum increments for the step-wise bidding curves. The step-wise bidding curves can expressed by the beakpoints: $B_{t}^{\mathrm{e,bu}} = \{(Q_{s,t}^{\mathrm{e,bu}}, m_{s,t}^{\mathrm{e}}) | \forall s \wedge Y_{s,t}^{\mathrm{e,bu}} = 1\}$, $B_{t}^{\mathrm{e,se}} = \{(Q_{s,t}^{\mathrm{e,se}}, m_{s,t}^{\mathrm{e}}) | \forall s \wedge Y_{s,t}^{\mathrm{se,bu}} = 1\}$ and $B_{t}^{\mathrm{reg,se}} = \{(Q_{s,t}^{\mathrm{reg,se}}, m_{s,t}^{\mathrm{reg,cap}}) | \forall s \wedge Y_{s,t}^{\mathrm{reg,se}} = 1\}$.

4) Scenario-based stochastic programming (SP): Overall, the optimal bidding of charging station in joint energy and frequency markets corresponds to the scenario-based SP:

$$\begin{aligned}
\max W = \max_{X} \sum_{s\in S} p_s \Big\{ &\sum_{t\in T} \left(W_{s,t}^{\mathrm{e,da}} + W_{s,t}^{\mathrm{e,rt}} - W_{s,t}^{\mathrm{e,penalty}}\right) \\
&+ \left(W_{s,t}^{\mathrm{reg,cap}} + W_{s,t}^{\mathrm{reg,perf}}\right) \Big\} \\
\text{s.t.} \quad &(1),(3),(4),(5),(6),(10),(11), \quad \forall s \in S.
\end{aligned} \tag{SP}$$

where X denotes the bidding strategy.

For problem (**SP**), a large number of scenarios is often required to fully characterize the multiple uncertainties. However, the computation burden grows rapidly with the number of scenarios. Scenario reduction or selection methods have been recognized as effective means to address the computational challenge. Nevertheless, most existing scenario reduction or selection methods focus on obtaining scenario subsets with minimal probability distance that share close statistical characteristics (i.e., mean and variance) to initial scenario set. These methods do not take into account the downstream SP and often lead to deficient bidding performance.

III. Problem-driven Scenario Reduction

To address the limitations, this paper proposes a problem-driven scenario reduction method for the optimal bidding of the charging station under uncertainty. The target is to select scenario subsets for the scenario-based (**SP**) to obtain bidding strategies with improved market performance while addressing the computational complexity. This method is in contrast to conventional scenario reduction methods and directly incorporate the downstream bidding optimization problem into scenario reduction The method consists of two

main procedures: problem-driven scenario representation and representation-based scenario reduction.

A. Problem-driven scenario representation

To begin with, we first investigate all the uncertain variables related to the optimal bidding of charging station. Specifically, for the scenario-based (**SP**), each scenario ξ_i is formed by market clearing price, solar generation, and vehicle charging and discharging flexibility, which can be expressed as

$$\begin{aligned}\xi_i := \Big\{ & \underbrace{m^{\mathrm{e}}_{i,t}, m^{\mathrm{e,rt}}_{i,\tau}, m^{\mathrm{reg,cap}}_{i,t}, m^{\mathrm{reg,perf}}_{s,t}}_{\text{Market clearing prices}}, \underbrace{P^{\mathrm{PV}}_{i,t}, P^{\mathrm{PV}}_{i,\tau}}_{\text{PV generation}}, \\ & \underbrace{P^{\mathrm{V2G,agg,ch,max}}_{i,\tau}, P^{\mathrm{V2G,agg,dis,max}}_{i,\tau} L^{\mathrm{V2G,agg,min}}_{i,\tau}, L^{\mathrm{V2G,agg,max}}_{i,\tau}}_{\text{Aggregated V2G charging flexibility}}, \\ & \underbrace{P^{\mathrm{EV,agg,ch,max}}_{i,\tau}, L^{\mathrm{EV,agg,min}}_{i,\tau}, L^{\mathrm{EV,agg,max}}_{i,\tau}}_{\text{Aggregated EV charging flexibility}} \Big\}, \forall \tau \in [t, t+\Delta t), t \in T.\end{aligned} \tag{12}$$

Each scenario corresponds to a high-dimensional matrix, i.e., $\xi_i \in \mathbb{R}^{13\times T_\tau}$, where 13 and T_τ are the total number of uncertain variables and daily real-time trading intervals. The scenario in (12) encapsulates all uncertainties that affect the scenario-based (**SP**) for the optimal bidding of charging station in joint energy and frequency markets.

To enable problem-driven scenario reduction, we move beyond traditional similarity measures defined in the original uncertainty space. Instead, we evaluate scenarios by their induced market outcomes. Specifically, for each scenario ξ_i, we solve the single scenario-based (**SP**):

$$\begin{aligned} X_i &= \arg\max_X \mathrm{VPP}(X, \xi_i), \quad \forall i \in S, \\ W_{ii} &= \max_X \mathrm{VPP}(X, \xi_i), \quad \forall i \in S, \end{aligned} \tag{13}$$

where $\mathrm{VPP}(X, \xi_i)$ denotes the scenario-based (**SP**) for the single scenario ξ_i. X_i and W_{ii} denotes the obtained optimal bidding strategy and bidding outcome. Notably, for the single-scenario scenario-based (**SP**), the step-wise bidding constraints (10)–(11) that involves a large number of binary variables and mixed-integer constraints can be omitted without affecting the optimal solutions. Because of that, the single-scenario (**SP**) are computationally efficient and will not contribute much computational burden to the proposed problem-driven scenario reduction method.

Once the bidding strategy X_i for scenario ξ_i is obtained, its behaviors (i.e., market performance) on any other scenario $\xi_j, j \in S$ can be evaluated by

$$W_{ij} = \mathrm{VPP}(X_i, \xi_j), \qquad \forall i \in S. \tag{14}$$

Accordingly, the behaviors of bidding strategy X_i on all involved scenarios $\boldsymbol{\xi}$ can be collectively captured by the following market performance vector:

$$\xi^c_i = \big[W_{i1}, W_{i2}, \cdots, W_{iS}\big], \quad \forall i \in S. \tag{15}$$

The vector ξ^c_i serves as a problem-aware representation of scenario ξ_i, as it captures how the strategy derived from ξ_i performs across all scenarios.

For two scenarios ξ_i and ξ_j, if their corresponding performance vectors ξ^c_i and ξ^c_j are close, it implies that the optimal bidding strategies X_i and X_j exhibit similar behaviors across the entire scenario set. Therefore, ξ_i and ξ_j can be regarded as equivalent in terms of their impact on the decision-making problem (**SP**). Based on this insight, we propose to perform scenario reduction in the space of market performance vectors $\{\xi^c_i\}_{i\in S}$ rather than in the original uncertainty space defined in (12). This enables the selection of representative scenarios that preserve decision-relevant characteristics, leading to more effective and economically meaningful scenario reduction.

It is worth noting that the problem-aware scenario representations $\xi^c = \{\xi^c_1, \xi^c_2, \cdots, \xi^c_S\}$ are only used to determine the indices of selected scenarios. Once the indices are determined, the corresponding original scenarios in ξ will input to problem scenario-based (**SP**) to obtain the step-wise bidding strategies.

B. Representation-based scenario reduction

Similar to conventional scenario reduction, a metric to quantify the distance between the original and the reduced scenario set is required for the problem-driven scenario reduction. In this study, the widely used Wasserstein distance is adopted to evaluate the distance between problem-aware scenario representation ξ^c and ζ^c. This corresponds to solving the following transport problem:

$$\begin{aligned} \mathrm{Dist}(\xi^c, \zeta^c) = \min_{\boldsymbol{\pi}} & \textstyle\sum_{i,j} d_{ij}\pi_{ij} \\ \text{s.t.} \quad & \textstyle\sum_j \pi_{ij} = p_i, \quad \sum_i \pi_{ij} = q_j, \quad \pi_{ij} \geq 0 \end{aligned} \tag{16}$$

where $d_{ij} = d(\xi^c_i, \zeta^c_j)$ represents a distance metric used to evaluate the similarity of scenario ξ^c_i and ζ^c_j. From the perspective of transport, $\boldsymbol{d} = [d_{ij}]$ and $\boldsymbol{\pi} = [\pi_{ij}]$ denote the distance and transport matrix. More specifically, π_{ij} denotes the probability of transporting from scenario ξ^c_i to scenario ζ^c_j and d_{ij} is the distance. The interpretation of Wasserstein distance is to measure the minimum transport cost of transferring from scenario set ξ^c to scenario set ζ^c.

When the two scenario sets $\boldsymbol{\xi}^c$ and $\boldsymbol{\zeta}^c$ are given, their Wasserstein distance can be obtained by solving the transport problem (16). However, in the context of scenario reduction, the reduced scenario set $\boldsymbol{\zeta}^c$ is unknown and needs to be determined. We therefore formulated the scenario reduction problem as

$$\begin{aligned} \boldsymbol{\zeta}^c = \arg \min_{\boldsymbol{\zeta}^c \subseteq \boldsymbol{\xi}^c, \boldsymbol{\pi} = [\pi_{ij}]} & \sum_{i,j} d_{ij}\pi_{ij} \\ \text{s.t.} \quad & \textstyle\sum_j \pi_{ij} = p_i, \quad \forall i \in S \\ & \pi_{ij} \geq 0, \quad \forall i \in S,\ j \in N. \end{aligned} \tag{SR}$$

where S and N represents the indices of original and reduced scenarios. For Problem (**SR**), both the reduced scenario set $\boldsymbol{\zeta}^c$ and the transport matrix $\boldsymbol{\pi} = [\pi_{ij}]$ are decision variables, which is essentially a combinatorial optimization problem. A common solution method is to introduce binary variables to indicate whether each original scenario is selected and included in the reduced set. This method is suitable for cases with a moderate size of original set. While this method is effective for problems with moderate size of original scenario set, it becomes computationally intractable for large-scale scenario sets due to the exponential growth of the search space.

To address this issue, an effective strategy is to relax the combinatorial constraints $\boldsymbol{\zeta}^c \subseteq \boldsymbol{\xi}^c$ and reformulate the problem as a scenario generation task. This relaxation transforms the original combinatorial problem into a continuous optimization problem and enables the use of gradient-based methods. Moreover, a recent work [26] shows that the transport matrix $\boldsymbol{\pi} = [\pi_{ij}]$ is often sparse, low-rank and non-smooth, which affects the effectiveness of gradient-based methods to approach the optimal solutions. An information entropy term for regulating the smoothness of transport matrix can be introduced to effectively improve the performance of gradient-based methods. This idea is adopted in this paper and we have the following regularized scenario reduction problem:

$$\boldsymbol{\zeta}^c = \arg\min_{\boldsymbol{\zeta}^c, \boldsymbol{\pi}=[\pi_{ij}]} \sum_{ij} d_{ij}\pi_{ij} - \varepsilon H(\pi) \qquad \textbf{(reg-SR)}$$

$$\text{s.t.} \quad \sum_j \pi_{ij} = p_i, \quad \forall i \in S. \tag{17a}$$

$$\pi_{ij} \geq 0, \quad \forall i \in S,\ j \in N. \tag{17b}$$

where $H(\boldsymbol{\pi})$ denotes the entropy of transport matrix $\boldsymbol{\pi} = [\pi_{ij}]$ and is defined as

$$H(\boldsymbol{\pi}) = \sum_{i,j} \pi_{ij} \log(1/\pi_{ij}) = -\sum_{i,j} \pi_{ij} \log(\pi_{ij}) \tag{18}$$

Note that a higher information entropy means a smoother transport matrix $\boldsymbol{\pi} = [\pi_{ij}]$ and vice versa. $\varepsilon \geq 0$ is a non-negative regularizer for trading off the Wasserstein distance and information entropy term. The objective of Problem (**reg-SR**) is to identify a scenario set $\boldsymbol{\zeta}^c$ and an associated transport matrix $\boldsymbol{\pi} = [\pi_{ij}]$ such that the distributional discrepancy with respect to the original scenario set $\boldsymbol{\xi}^c$ is minimized, while ensuring sufficient smoothness of transport matrix $\boldsymbol{\pi} = [\pi_{ij}]$ to facilitate effective optimization.

According to [26], another benefit of the information entropy term is that it enables a convex optimization problem and Problem (**reg-SR**) can be converted into an unconstrained optimization problem based on strong duality theorem. Specifically, by relaxing (17a), we have the Lagrangian function:

$$L(\boldsymbol{\lambda}, \boldsymbol{\zeta}^c, \boldsymbol{\pi}) = \sum_{i,j} d_{ij}\pi_{ij} - \varepsilon H(\boldsymbol{\pi}) + \sum_i \lambda_i \left(\sum_j \pi_{ij} - p_i\right) \tag{19}$$

where $\boldsymbol{\lambda} = [\lambda_1, \lambda_2, \cdots, \lambda_S]$ are Lagrangian multipliers associated with the constraints $\sum_j \pi_{ij} = p_i, \forall i \in S$.

The optimal Karush–Kuhn–Tucker (KKT) conditions are

$$\partial L/\partial \pi_{ij} = d_{ij} + \varepsilon \log \pi_{ij} + \lambda_i = 0, \tag{20a}$$

$$\partial L/\zeta_j^c = \sum_i \partial\left(d_{ij}\pi_{ij}\right)/\partial \zeta_j^c = 0, \tag{20b}$$

$$\partial L/\partial \lambda_i = \sum_j \pi_{ij} - p_i = 0, \quad \forall i \in S, j \in N. \tag{20c}$$

According to (20a), the optimal solution $(\boldsymbol{\zeta}^{c,*}, \boldsymbol{\pi}^*, \boldsymbol{\lambda}^*)$ of Problem (**reg-SR**) satisfies

$$\pi_{ij}^* = \exp\left(\frac{-d_{ij}^* - \lambda_i^*}{\varepsilon}\right) = \exp\left(-\frac{\lambda_i^*}{\varepsilon}\right)\exp\left(-\frac{d_{ij}^*}{\varepsilon}\right) = u_i^* k_{ij}^*, \tag{21}$$

where we define $u_i^* = \exp(-\lambda_i^*/\varepsilon)$ and $k_{ij}^* = \exp(-d_{ij^*}/\varepsilon)$. Further, substituting (21) into (20c) yields

$$u_i^* \sum_j k_{ij}^* = p_i \rightarrow u_i^* = p_i / \sum_j \exp(-d_{ij}^*/\varepsilon). \tag{22}$$

Substituting (22) into (21), we have:

$$\pi_{ij}^* = u_i^* k_{ij}^* = p_i \cdot \frac{\exp(-d_{ij}^*/\varepsilon)}{\sum_j \exp(-d_{ij}^*/\varepsilon)}. \tag{23}$$

where it is worth noting that we directly have $\pi_{ij}^* \in (0,1)$, satisfying the non-negative property of transport matrix. That is why we dot not need to relax the constraints (17b) in (19).

With the analytical solution (23), Problem (**reg-SR**) can be converted into an unconstrained optimization problem:

$$\boldsymbol{\zeta}^{c,*} = \arg\min_{\boldsymbol{\zeta}^{c,*}} \left(\sum_{i,j} d_{ij}^* \pi_{ij}^* + \varepsilon \sum_{i,j} \pi_{ij}^* \log(\pi_{ij}^*)\right) \tag{24}$$

where π_{ij}^* is uniquely determined by d_{ij}^* as shown in (23) and $\boldsymbol{\zeta}^{c,*}$ is thus the only decision variable to be optimized.

Gradient-based methods can be directly applied to solve the Problem (24). Generally, we first initialize the scenario set $\boldsymbol{\zeta}^{c,*}$ to be a matrix, we then update $\boldsymbol{\zeta}^{c,*}$ by a gradient-based method in an iterative manner. At each iteration, the distance matrix is first evaluated by $d_{ij} = d(\xi_i^c, \zeta_j^{c,*})$, and the transport matrix $\boldsymbol{\pi}^* = [\pi_{ij}^*]$ is then calculated by (23).

By leveraging the automatic differentiation framework provided by neural network libraries, the optimization problem is solved via backpropagation implemented in PyTorch. Specifically, a neural network is constructed in which the reduced scenario set $\boldsymbol{\zeta}^{c,*}$ is treated as a set of trainable parameters and is iteratively updated to minimize the training loss:

$$L_{\text{loss}} = \sum_{i,j} d_{ij}\pi_{ij}^* + \varepsilon \sum_{i,j} \pi_{ij}^* \log \pi_{ij}^* \tag{25}$$

The above approach generates a set of scenarios from the original one. The next step is to map each scenario in $\boldsymbol{\zeta}^{c,*}$ to that in the original scenario set $\boldsymbol{\xi}^c$. This can be achieved by selecting the closest scenario in the original scenario set. Formally, for each $\zeta_i^{c,*} \in \boldsymbol{\zeta}^{c,*}$, the closest scenario $\xi_j^c \in \boldsymbol{\xi}^c$ is

$$\zeta_j^c = \arg\min_{\zeta_j^c \in \boldsymbol{\xi}^c} d(\zeta_j^{c,*}, \zeta_j^c), \quad \forall j \in N. \tag{26}$$

We therefore obtain a scenario subset $\boldsymbol{\zeta}^c = [\zeta_1^c, \zeta_2^c, \cdots, \zeta_N^c]$ of original scenario set $\boldsymbol{\xi}^c$. Further, the associated probability distribution $Q = [q_1, q_2, \ldots, q_N]$ can be obtained by

$$\begin{aligned} &q_j = \sum_{i \in C_j} p_i, \\ &C_j = \left\{ i \in S | j = \arg\min_{\zeta_j^c \in \boldsymbol{\zeta}^{c,*}} d(\xi_i^c, \zeta_j^c) \right\} \quad j \in N. \end{aligned} \tag{27}$$

where $C_j \subseteq S$ denotes the indices of scenarios in the original set that are closest to the reduced scenario ζ_j^c. It is straightforward that $\sum_j q_j = 1$ given $\sum_i p_i = 1$. The overall architecture of the proposed problem-driven scenario reduction method for VPP bidding are summarized in Fig. 2.

IV. Case Studies

This section evaluates the performance of charging station participating in electricity markets based on the proposed bidding model and problem-driven scenario reduction method. Particularly, we consider a solar-integrated charging station with both EVs and V2Gs jointly participating in energy and frequency markets. For scenario reduction, we comparatively investigate the following methods:

- **Random scenario reduction:** Scenario subsets of size N are randomly sampled from the original one $\xi = \{\xi_1, \xi_2, \cdots, \xi_S\}$. To account for sampling variability, 60 subsets are sampled.
- **Data-based scenario reduction:** The original scenario set $\boldsymbol{\xi} = \{\xi_1, \xi_2, \cdots, \xi_S\}$ is directly used for scenario reduction, corresponding to conventional scenario reduction.

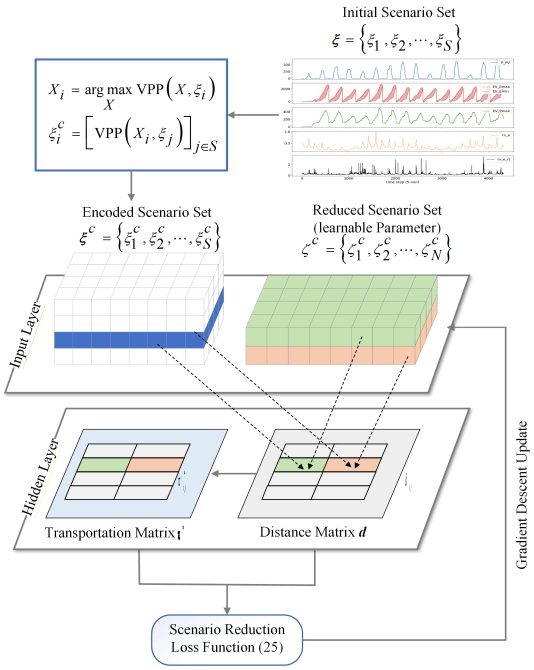

Fig. 2. Problem-driven scenario reduction for VPP bidding.

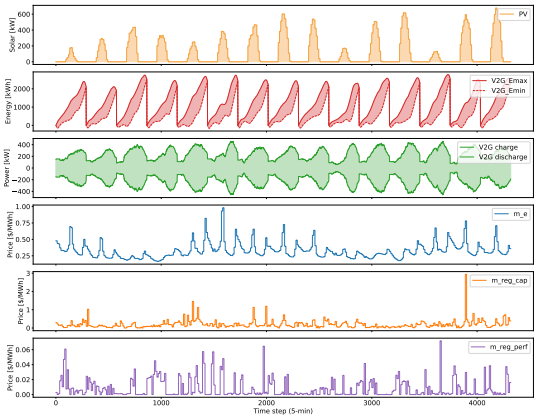

Fig. 3. Solar power, electric vehicle charging demand, market prices

This is implemented by directly replacing $\boldsymbol{\xi}^c$ by $\boldsymbol{\xi}$ with the proposed scenario reduction method.

- **Problem-driven scenario reduction:** Selecting scenarios by the problem-ware scenario representation $\boldsymbol{\xi}^c = \{\xi_1^c, \xi_2^c, \cdots, \xi_S^c\}$ instead of the original scenario set, corresponding to the proposed problem-driven scenario reduction method.

A. Datasets and configuration

Case studies are conducted based on real world datasets.

1) Solar Power: The solar power generation is adopted from the historical observations of two solar power plants in India with a temporal resolution of 15 seconds and spanning from 2020/5/15 to 2020/6/17 [27].

2) Electric Vehicles: The uni-directional EV and bi-directional V2G charging demand is obtained from an open EV charging dataset comprising 2,337 EV users, 2,119 charging stations, and 72,856 charging sessions from 2021/9/30 to 2022/9/30 [28]. Each charging session includes arrival time, departure time, parking duration and charging demand, which can be directly used to obtain the aggregated bidding models according to our previous work [25].

3) Market Prices: The PJM electricity market in US is considered in this paper. Historical prices are directly downloaded from its official website [29], including day-ahead and real-time energy market prices, as well as frequency capacity and performance prices. The price data covers approximately 3 months (90 days) and consists of two non-consecutive periods (2023/12/8-2024/1/15 and 2024/2/11-2024/4/1).

We resample and align the datasets to a unified temporal resolution (5 mins) and length (90 days). We then divide the datasets by a ratio of 7:2, where 70 days of data are used to obtain the optimal bidding strategies based on the scenario-based SP approach and the other 20 days are used for testing the market performance of bidding strategies. The testing corresponds to market clearing process. More specifically, the quantities for each trading interval is determined by comparing the realized market clearing price and the obtained step-wise bidding curves. The maximum daily number of parked vehicles at the station is 317. We set the maximum number of allowable quantify-price pairs of step-wise bidding curves for both energy and frequency markets as 15. Euclidean distance is used as the distance metric of scenarios.

B. Computational Complexity

Before performing scenario reduction, we first investigate how the number of scenarios used for the scenario-based (**SP**) affects both the computation time and market performance of resulting bidding strategies for the charging station. We randomly sample scenario subsets from the original one ($S = 70$) of sizes ranging from 5 to 30 with a stepsize of 5. For each scenario subset size, 10 independent subsets are sampled and each of them is used in the scenario-based (**SP**) to obtain the bidding strategies which are then tested on the 20-day dataset. The average solving time and the resulting market payment (i.e., negative revenue) of different scenario sizes are reported in TABLE I. The performance gap is evaluated by the average market payment based on the results of scenario size 30. We first observe that as the scenario size increases, the market payment consistently decreases across the cases. This implies that an increasing number of scenarios for uncertainty representation generally leads to improved bidding strategies. However, the improvements are achieved at the cost of a rapidly increasing computational burden as reflected by the solving time. Besides, from the results, we find that the performance gap for the scenario sizes 10-20 is less 7% and the solving time is approximately within 10 mins, which provide a favorable trade-off between the market performance and the computation efficiency. We therefore set the reduced scenario size as $N = 10$ and $N = 20$ for the following case studies.

TABLE I
COMPUTATIONAL COMPLEXITY AND MARKET PERFORMANCE OF BIDDING STRATEGIES WITH DIFFERENT SCENARIO SIZES.

Scenario Size	5	10	15	20	25	30
Solving Time [s]	3.97	51.36	163.04	352.42	609.00	1193
Market payment [$]	814.08	663.83	657.27	652.14	620.50	619.41
Perf. Gap [%]	**31.4**	**7.2**	**6.1**	**5.2**	**0.2**	**–**

C. Market performance

This section evaluates the market performance of obtained bidding strategies for the charging station. We consider case

TABLE II
MARKET PERFORMANCE OF CHARGING STATION BIDDING IN ELECTRICITY MARKETS USING DIFFERENT SCENARIO REDUCTION METHODS

Scenarios size	**Case**	**Vehicles**	**Markets**	**Average daily market payment [$]**			**Improvement [%]**	
				Problem-driven	Data-based	Random	Problem–Data	Problem–Random
$N = 10$	Case 1	EVs	Energy	**594.52**	667.85	640.20	10.98	7.14
	Case 2	V2Gs	Energy	**638.50**	666.95	678.63	4.26	5.91
	Case 3	EVs + V2Gs	Energy	**1221.73**	1320.84	1303.50	7.50	6.27
	Case 4	EVs	Energy + Freq	**312.11**	398.51	378.97	21.68	17.64
	Case 5	V2Gs	Energy + Freq	**291.34**	353.50	341.79	17.59	14.80
	Case 6	EVs + V2Gs	Energy + Freq	**663.83**	763.90	733.04	13.10	9.44
$N = 20$	Case 7	EVs	Energy	**572.46**	661.16	646.23	13.40	11.43
	Case 8	V2Gs	Energy	**602.24**	696.03	686.41	13.48	12.25
	Case 9	EVs + V2Gs	Energy	**1207.73**	1268.44	1290.83	4.79	6.44
	Case 10	EVs	Energy + Freq	**311.07**	383.51	373.82	18.90	16.79
	Case 11	V2Gs	Energy + Freq	**272.68**	351.19	336.82	22.36	19.05
	Case 12	EVs + V2Gs	Energy + Freq	**631.31**	715.50	689.47	11.77	8.44

studies where the charging station participates in either energy market or the joint energy and frequency markets. Besides, we consider the charging station involving EVs, V2Gs or their both in the case studies. Three scenario reduction methods (i.e., **Problem-driven**, **Data-based**, **Random**) are used to obtain scenario subsets of size 10 and 20 for the scenario-based (**SP**). For each case, we first obtain a reduced scenario set, which is then used for the scenario-based (**SP**) to obtain the bidding strategy. The market performance of the bidding strategies are evaluated on the 20-day dataset by executing the market clearing process. For the random scenario reduction, 60 scenario subsets are sampled to account for the sampling variability and each of them is used for computing bidding strategies. Since the charging station is an energy consumer, we use market payment (negative revenue) as performance metric. The average daily market payment of the charging station for each case is evaluated. The results of all case studies are reported in TABLE II.

The results show that the proposed problem-driven scenario reduction method consistently outperforms the other two approaches across all case studies. Specifically, it provides approximately 10-20% market performance improvement over the data-based and random scenario reduction methods for most case studies. This demonstrates that by incorporating downstream scenario-based (**SP**) into scenario reduction, the problem-driven scenario reduction method is able to improve the bidding strategies. Further, by comparing the results of scenario size 10 and 20, we conclude that the increased number of scenarios leads to improved bidding strategies as indicated by Case 1-6 and Case 7-12. This is consistent with the results presented in TABLE I. This is reasonable as a larger number of scenarios can generally better capture the multiple uncertainties. However, the improvements will be achieved at the cost of increasing computational burden as indicated in TABLE I. Besides, the results show that the joint energy and frequency market participation can significantly enhance the market revenue of the charging station. Specifically, by inspecting the results with the proposed problem-driven method, we find that the market payment is reduced by over 45% for all case studies.

The improved market performance of proposed problem-driven scenario method can be further perceived from the distributions of daily market payment shown in Fig.4. The first 10 days of daily market payment under the different scenario reduction methods are presented. The transparent bars above and below the X-axis indicate energy market payment and frequency market payment (i.e., revenue), respectively. The shaded bars indicate the overall market payment. For the random scenario reduction method, the daily market payment is averaged across the 60 scenario subsets for each day. The results show that the problem-driven scenario-reduction method yields reduced market payment for almost all days.

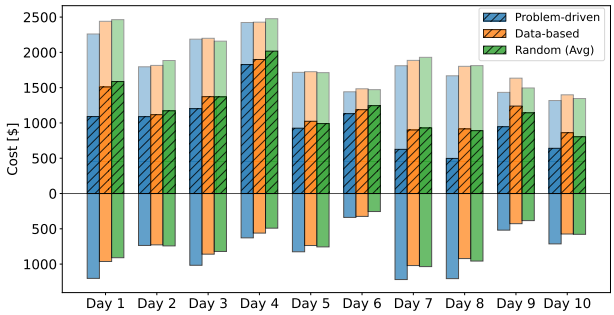

Fig. 4. Distributions of daily market payment of charging station for Case 6

D. Step-wise bidding strategies

This section investigates the bidding strategies obtained from the scenario-based SP. Particularly, this paper considers constructing step-wise bidding strategies to hedge against the effects of the multiple uncertainties. This section evaluates whether the three properties (i.e., **monotonicity**, **nonanticipativity**, and **segment limits**) are provided by the obtained bidding strategies.

We use **Case 6** as an example where the charging station involves both EVs and V2Gs participating in the joint energy and frequency markets. The obtained step-wise bidding strategies for day-ahead energy and frequency markets across all trading intervals are presented in Fig. 5. The results show that the bidding strategy for each trading interval is composed of different number of stair-wise segments, which is to our expectation. However, for most trading intervals the number of segments is much smaller than the maximum allowable limits 15. This is mainly because for such trading intervals the bidding outcome is not sensitive to the market clearing prices. Besides, it is obvious that all the step-wise bidding

curves satisfy the monotonicity and segment limits properties. Specifically, all buying curves satisfy the non-increasing properties w.r.t the market price and vice versa with all selling curves. It is worth noting that the nonanticipativity is hard to identify visually and thus not discussed here.

In addition, we find that for most trading intervals, the charging station bids to buy instead of sell in day-ahead energy market. This is because the on-site solar generation is not sufficient to satisfy the charging demand and the station acts as an energy consumer in the market. However, for frequency markets, the charging station bids to sell capacity for almost all trading intervals. This is reasonable as there exist substantial flexibility both from the charging demand and the energy storage capacity of V2Gs can be utilized to gain profit from the frequency market.

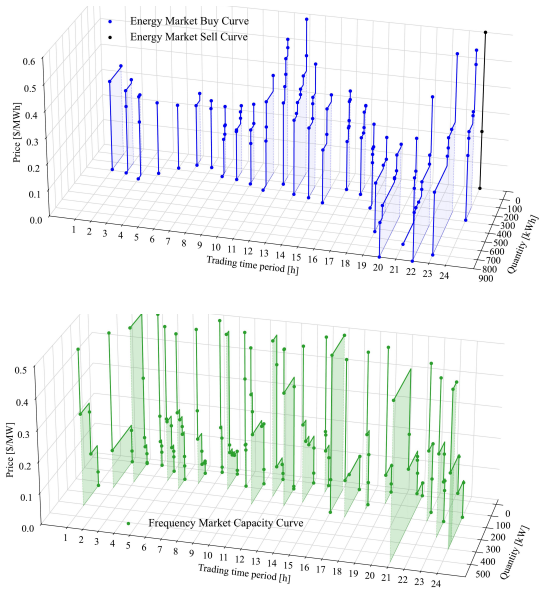

Fig. 5. Step-wise bidding curves of charging station for Case 6.

E. Intuition of problem-driven scenario reduction

In this section, we try to give some intuitive insight on the rationale of the problem-driven scenario reduction considering the difficulty to conduct theoretical analysis.

To achieve the objective, we randomly sample a scenario subset of size 20 from the original one ($S = 70$). We then evaluate their pairwise similarity of the scenario subset by the Gaussian similarity measure:

$$S_{ij} = exp(-d_{ij}^2/(2\sigma^2)), \forall i, j \in N \tag{28}$$

where N denotes the indices of selected scenarios.

Particularly, for each pair of scenarios, both the original scenario representation (i.e., ζ_i, ζ_j) and the problem-aware representation (i.e., ζ_i^c, ζ_j^c) are used for evaluating the Gaussian similarity, respectively. This actually can reveal the difference of data-based and problem-driven scenario reduction methods.

Based on the obtained results, we visualize the pair-wise similarity of the scenario subset in heat map in Fig. 6. Each square of the heat map is used to represent the similarity of a pair of scenarios, where a darker color indicates higher similarity. The white square A and B is a local zooming of pair-wise similarity for scenario $12, 13, 14$.

It can be observed from the results that the similarities of data-based scenario representation are highly diverse and we do not observe obvious patterns across the scenarios. This is mainly caused by the multiple uncertainties. Whereas for problem-driven scenario representation, many of the scenarios show high similarities. From the results, we find that the distribution of pair-wise scenarios are quite different between the data-based and problem-driven methods. More specifically, the pair-wise scenario similarities of data-based method are highly diverse and no obvious patterns are observed. However, the problem-driven method lead to much structured distributions of the pair-wise scenario similarities. This is because the optimal bidding strategies of charging station are affected by the multiple uncertainties (i.e., solar generation, vehicle charging flexibility, and the market clearing prices). They have collective impacts on the resulting bidding strategies. As a result, though the scenarios formed by the multiple uncertain variables as expressed in (12) varies, they may lead to similar solution of the downstream scenario-based (**SP**). That is why we observe block-wise high similarity (i.e., close to 100) from the results of the problem-driven method. This above results provide an intuitive explanation for the effectiveness of the proposed problem-driven scenario reduction method for the optimal bidding of charging station in electricity market.

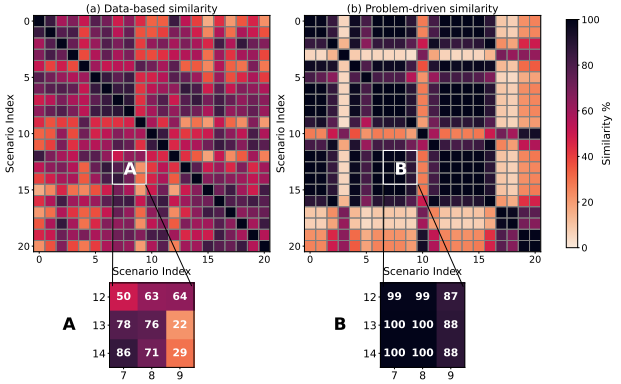

Fig. 6. Pair-wise similarity of scenarios with data-based and problem-driven scenario reduction

V. Conclusion

This paper investigated the optimal bidding of a solar-integrated charging station in joint energy and frequency market under uncertainty. A multi-time-scale aggregated bidding model that accounts for the temporal and hierarchical couplings of joint market participation and the large number of vehicles was established. Step-wise bidding curves to hedge against the multiple uncertainties were optimized based on scenario-based stochastic programming (SP). To address the computational challenge associated with scenarios used for capturing the multiple uncertainties, we proposed a problem-driven scenario reduction method to guide the informed scenario selection for the downstream bidding optimization problem. Case studies based on real-world datasets demonstrated the proposed scenario reduction method can improve the market performance of the charging station by approximately 10-20% compared with conventional scenario reduction methods. Besides, the results indicated that the joint energy and frequency market participation can significantly improve the economic benefit of the charging station (i.e.,

over 45%) compared with pure energy market participation. Some intuitive insights regarding the problem-driven scenario reduction method were illustrated. The results implied that the proposed problem-driven method is able to capture the collective impacts of the multiple uncertainties on the downstream bidding problem and thus improve the bidding strategies, which are not provided by the conventional scenario reduction method.

REFERENCES

[1] International Energy Agency, "Global ev outlook 2025," 2025. Licence: CC BY 4.0.

[2] PJM Interconnection, "Advanced Technology: Exploring Tomorrow's Grid," 2023. https://www.pjm.com/-/media/DotCom/about-pjm/exploring-tomorrows-grid/advanced-tech.pdf.

[3] The Mobility House North America, "The Mobility House North America Launches Cascade EV Aggregator," 2026. https://www.mobilityhouse.com/usa_en/our-company/newsroom/article/cascade-ev-aggregator-launch.

[4] ev.energy, "California CCAs Partner with ev.energy to Create Statewide Virtual Power Plant," 2024. https://www.ev.energy/blog/california-ccas-partner-with-ev-energy-to-create-statewide-virtual-power-plant.

[5] D. Matkovic, T. M. Pilski, and T. Capuder, "Participation of electric vehicle charging station aggregators in the day-ahead energy market using demand forecasting and uncertainty-based pricing," *Energy*, vol. 328, p. 136299, 8 2025.

[6] Z. Wang, J. Gao, R. Zhao, J. Wang, and G. Li, "Optimal bidding strategy for virtual power plants considering the feasible region of vehicle-to-grid," *Energy Conversion and Economics*, vol. 1, no. 3, pp. 238–250, 2020.

[7] Á. García-Cerezo, L. Baringo, D. Bonilla, and J. García-González, "Building bidding curves for an EV aggregator via stochastic adaptive robust optimization," in *2024 International Conference on Smart Energy Systems and Technologies (SEST)*, pp. 1–6, IEEE, 2024.

[8] Á. García-Cerezo, L. Baringo, and J. García-González, "A stochastic adaptive robust optimization approach to build day-ahead bidding curves for an EV aggregator," *IEEE Transactions on Industry Applications*, vol. In press, pp. 1–10, 2025.

[9] D. Chen, Z. Jing, and H. Tan, "Optimal bidding/offering strategy for ev aggregators under a novel business model," *Energies*, vol. 12, no. 7, p. 1384, 2019.

[10] S. Sadeghi, H. Jahangir, B. Vatandoust, M. A. Golkar, A. Ahmadian, and A. Elkamel, "Optimal bidding strategy of a virtual power plant in day-ahead energy and frequency regulation markets: A deep learning-based approach," *International Journal of Electrical Power & Energy Systems*, vol. 127, p. 106646, 2021.

[11] S. Gao, R. Dai, W. Cao, and Y. Che, "Combined provision of economic dispatch and frequency regulation by aggregated evs considering electricity market interaction," *IEEE Transactions on Transportation Electrification*, vol. 9, no. 1, pp. 1723–1735, 2023.

[12] M. Song and M. Amelin, "Purchase bidding strategy for a retailer with flexible demands in day-ahead electricity market," *IEEE Transactions on Power Systems*, vol. 32, no. 3, pp. 1839–1850, 2016.

[13] R. Herding, E. Ross, W. R. Jones, V. M. Charitopoulos, and L. G. Papageorgiou, "Stochastic programming approach for optimal day-ahead market bidding curves of a microgrid," *Applied Energy*, vol. 336, 2023.

[14] R. Herding, E. Ross, W. R. Jones, E. Endler, V. M. Charitopoulos, and L. G. Papageorgiou, "Risk-aware microgrid operation and participation in the day-ahead electricity market," *Advances in Applied Energy*, vol. 15, p. 100180, 2024.

[15] X. Xiao, J. Wang, R. Lin, D. J. Hill, and C. Kang, "Large-scale aggregation of prosumers toward strategic bidding in joint energy and regulation markets," *Applied Energy*, vol. 271, p. 115159, 2020.

[16] H. J. Kim and M. K. Kim, "Data-driven virtual power plant bidding strategy in electricity markets integrating hybrid forecasting model and customized incentive demand response," *IEEE Internet of Things Journal*, 2025.

[17] F. Fang, S. Yu, and X. Xin, "Data-driven-based stochastic robust optimization for a virtual power plant with multiple uncertainties," *IEEE Transactions on Power Systems*, vol. 37, no. 1, pp. 456–466, 2021.

[18] H. Heitsch and W. Römisch, "Scenario reduction algorithms in stochastic programming," *Computational Optimization and Applications*, vol. 24, no. 2-3, pp. 187–206, 2003.

[19] H. Heitsch and W. Römisch, "Scenario reduction algorithms in stochastic programming," *Mathematical Programming*, vol. 101, no. 1, pp. 125–148, 2004.

[20] J. Dupačová, N. Gröwe-Kuska, and W. Römisch, "Scenario reduction in stochastic programming," *Mathematical programming*, vol. 95, pp. 493–511, 2003.

[21] X. Zhao, Y. Li, and J. Wang, "Scenario generation and reduction in stochastic programming: A review," *Applied Energy*, vol. 288, p. 116634, 2021.

[22] X. Chou and E. Messina, "Problem-driven scenario generation for stochastic programming problems: a survey," *Algorithms*, vol. 16, no. 10, p. 479, 2023.

[23] Y. Zhuang, L. Cheng, N. Qi, M. R. Almassalkhi, and F. Liu, "Problem-driven scenario reduction framework for power system stochastic operation," *IEEE Transactions on Power Systems*, 2024.

[24] I. Suemitsu and K. Izui, "Surrogate-assisted scenario-generation method for simulation-based stochastic programming problems," *IEEE Transactions on Automation Science and Engineering*, 2025.

[25] B. Zhao, Y. Yang, Q.-S. Jia, Y. Yang, and X. Guan, "A generalized virtual energy storage model for efficient electric vehicle charging flexibility characterization and aggregation," 2026. Available: https://yangyu-bears-berkeley.github.io/pdf/V2G_Agg_short_updated_full.pdf.

[26] X. Dong, Y. Wang, Z. Chen, and Y. Li, "Scenario reduction network based on wasserstein distance with regularization," *IEEE Transactions on Power Systems*, vol. 38, no. 5, pp. 4309–4321, 2023.

[27] Kaggle, "Solar power generation data." https://www.kaggle.com/datasets/anikannal/solar-power-generation-data, 2025. Accessed: October 3, 2025.

[28] K. Baek, E. Lee, and J. Kim, "A dataset for multi-faceted analysis of electric vehicle charging transactions," *Scientific Data*, vol. 11, no. 1, p. 262, 2024.

[29] PJM Interconnection, "Daily Energy Market Offer Data (Unit Bid)," 2026. Accessed: 2026-02-06; Historical offer data for generation units in PJM energy market, with details on bid curves and unit characteristics.